

Supplementary Materials (Supplementary Figures)

Protein Kinase 2 of the Giant Sarcomeric Protein UNC-89 Regulates Mitochondrial Morphology and Function

Yohei Matsunaga¹, Hiroshi Qadota¹, Nasab Ghazal², Leila Lesanpezeshki³, Till Dorendorf⁴, Jasmine C. Moody¹, Arnaud Ahier⁵, Courtney J. Matheny¹, Siva A. Vanapalli³, Steven Zuryn⁵, Olga Mayans⁴ Jennifer Q. Kwong², Guy M. Benian^{1*}

¹ Department of Pathology, Emory University, Atlanta, Georgia 30322 USA

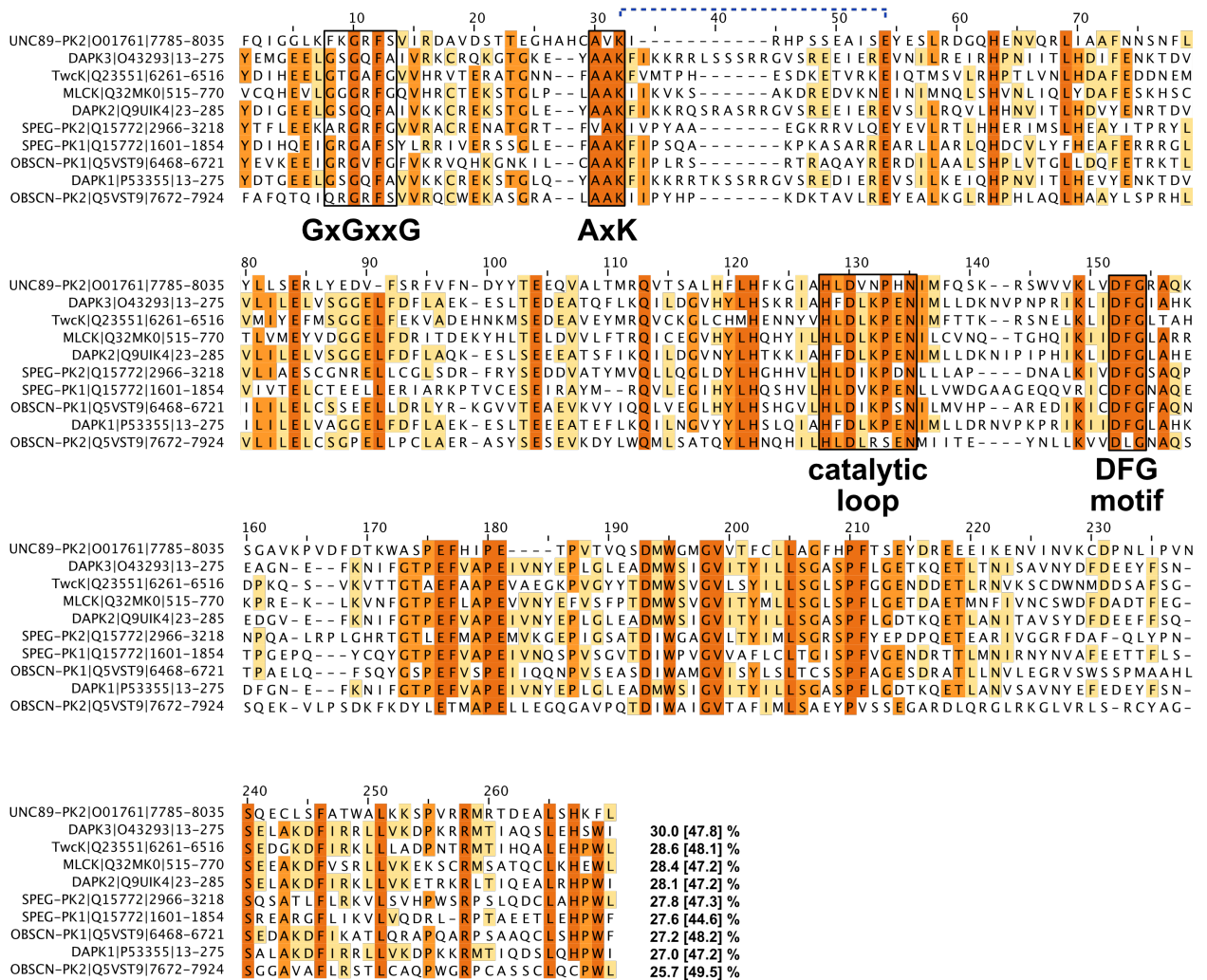
² Department of Pediatrics, Emory University, Atlanta, Georgia 30322 USA

³Department of Chemical Engineering, Texas Tech University, Lubbock, Texas 79409 USA

⁴Department of Biology, University of Konstanz, 78457 Konstanz, Germany

⁵Clem Jones Centre for Ageing Dementia Research, Queensland Brain Institute, The University of Queensland, Brisbane, QLD 4072, Australia

*corresponding author, pathgb@emory.edu



Supplementary Figure 1. UNC-89-PK2 is most similar to muscle kinases and cytoskeleton-associated kinases from the DMT clade of the CAMK family

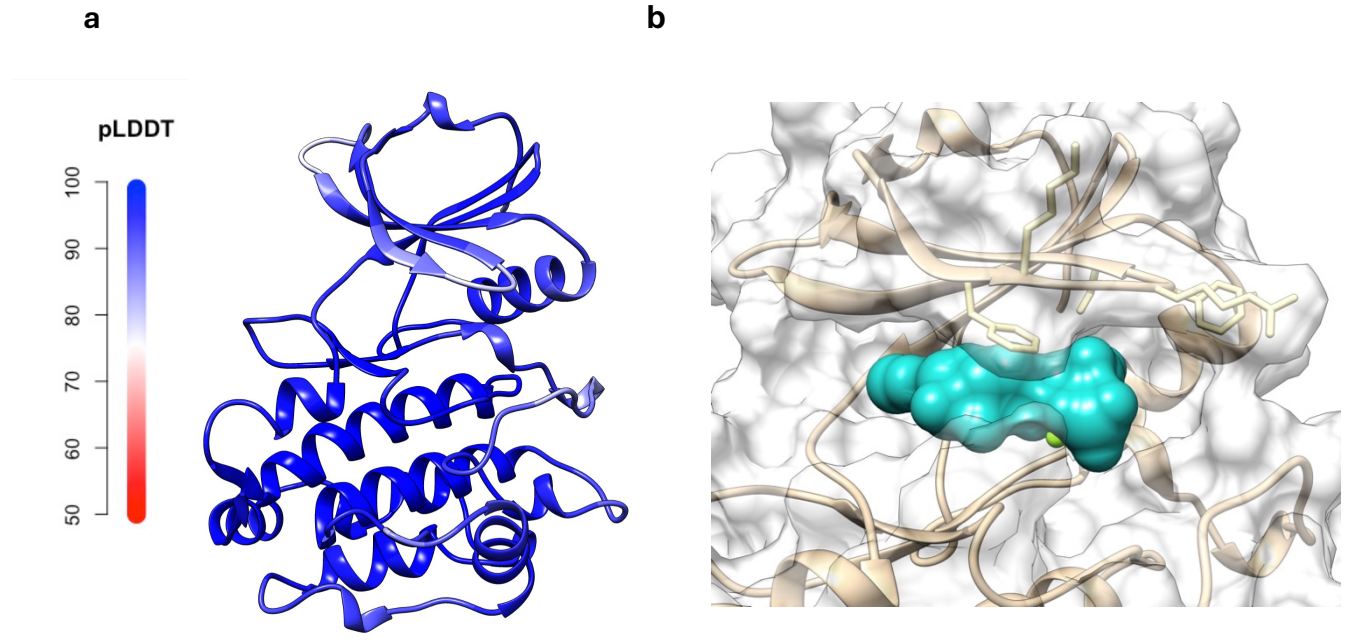
Sequence alignment of UNC-89-PK2 with its most closely related human kinases (identified using BLAST; <https://blast.ncbi.nlm.nih.gov>) as well as the well studied twitchin kinase (Twck) from *C. elegans* muscle. For all sequences, kinase name, UniProtKB code and protein residue range are given.

Catalytically relevant motifs (marked) are conserved. The salt bridge formed by the strictly conserved lysine and glutamate residues that defines the catalytically committed state of canonical kinases is indicated with a blue dashed line. For each kinase, pair-wise sequence identity to UNC-89-PK2 is given and sequence conservation is in square brackets.

		GxGxxG
Nematodes	Caenorhabditis_elegans	F K G R F S
	Necator_americanus	F K G K Y S
	Diploscapter_pachys	F K G R F S
	Pristionchus_pacificus	A R G R F A
Insects	Drosophila_melanogaster	A R G E F S
	Bombus_impatiens	S R G Q F S
	Apis_mellifera	Y R G Q F S
	Camponotus_floridanus	S Q G Q F S
Mammals	Homo_sapiens	Q R G R F S
	Pongo_abelii	R R G R F S
	Vulpes_lagopus	R R G R F S
	Equus_quagga	R R G R F S
	Choloepus_didactylus	W R G R F S
	Sus_scrofa	R R G R F S
	Orcinus_orca	R R G R F S
	Mus_musculus	R R G R F S
	Xenopus_laevis	K R G R F S
	Crotalus_tigris	K R G R F S
Birds	Lagopus_leucura	K R G R F S
	Gallus_gallus	K R G R F S
	Falco_rusticolus	K R G R F S
Fish	Danio_rerio	N R G R F S
	Esox_lucius	N R G R F S

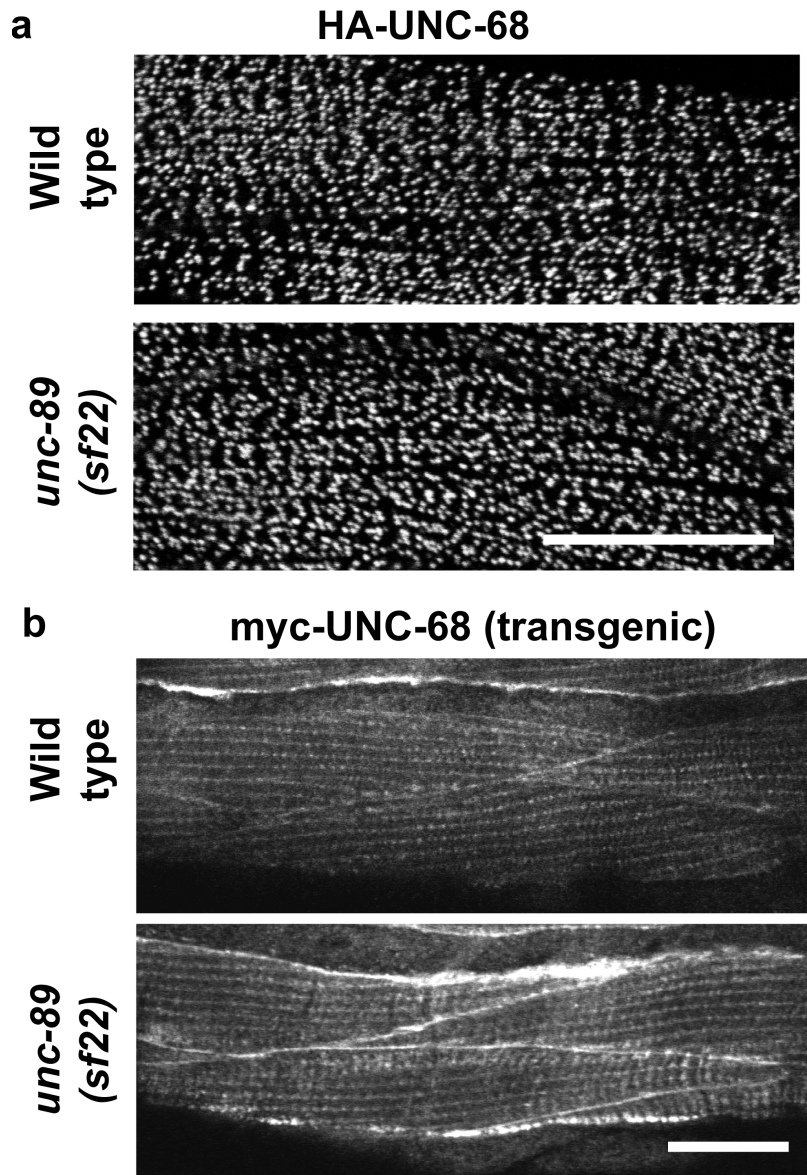
Supplementary Figure 2. Sequence composition of the ATP-binding glycine rich motif in PK2 kinases from UNC-89 (obscurin) proteins across phylogenetic animal groups.

In PK2 kinases, the canonical GxGxxG motif adopts the form LxGxxS, where L stands for large, bulky residue. Low conservation of position 1 in this motif is common across kinases and it is known not to conflict ATP binding or phosphotransfer activity. For example, within this group, mouse obscurin PK2 (containing an arginine residue as this position) has been shown to phosphorylate N-cadherin *in vitro*¹.



Supplementary Figure 3. 3D-modelling of UNC-89-PK2 and its binding of ATP

a. Cartoon representation of the 3D-model (model 0) calculated with AlphaFold (as described in Methods, main text). Coloring indicates the confidence of the prediction expressed as a per-residue Local Distance Difference Test (pLDDT) (scale indicated in the gradient bar; left). The model of the kinase sequence was considered to have been confidently predicted, with regions with a pLDDT below 70 (deemed unreliably) not being present in the model. b. Model of UNC-89-PK2 in complex with ATP (cyan surface) and magnesium (green ion). The residues forming the ATP-binding LxGxxS β -hairpin loop of UNC-89-PK2 are explicitly shown. The model was constructed by direct superimposition of the AlphaFold model of UNC-89-PK2 with the crystal structure of human DAPK1 kinase (PDB code 3F5U), which is complexed to the ATP-analog AMPPNP and Mg²⁺. The location of AMPPNP/Mg²⁺ resulting from this simple superimposition is directly compatible with binding into the ATP pocket of UNC-89-PK2, suggesting that UNC-89-PK2 can productively bind ATP/Mg²⁺ in a fashion that resembles that of DAPK1.

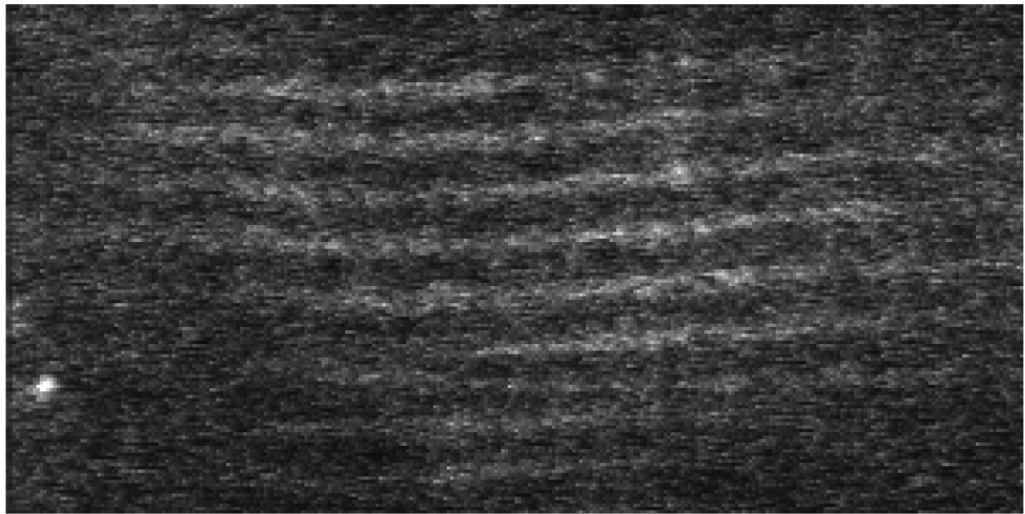


Supplementary Figure 4. The PK2 KtoA mutation does not affect the structure of the sarcoplasmic reticulum (SR).

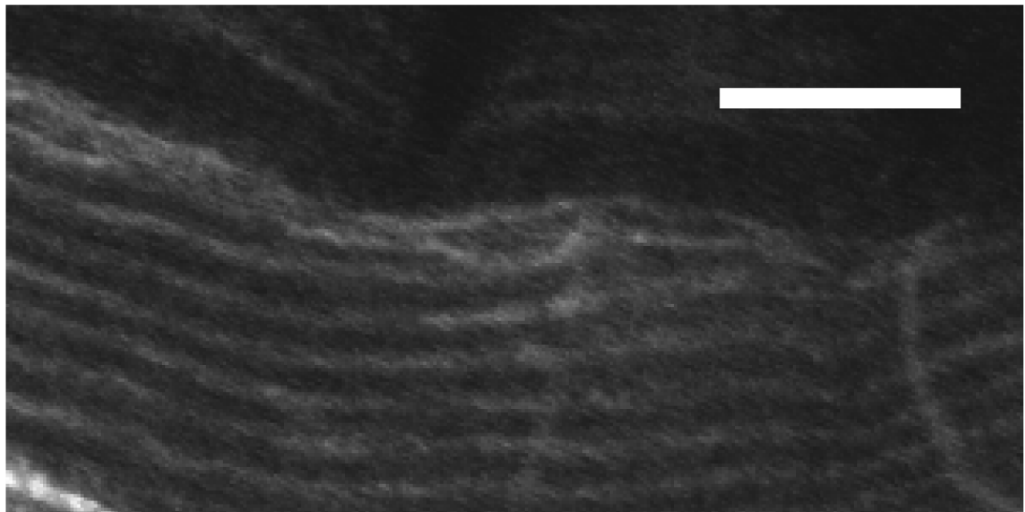
a. UNC-68 (ryanodine receptor) was endogenously expressed with an N-terminal HA tag generated by CRISPR/Cas9, and imaged using antibodies to HA and confocal microscopy. b. UNC-68 with an N-terminal myc tag, was overexpressed from a transgene, and imaged using antibodies to myc. With either method, there is no discernible difference in localization of UNC-68, or by proxy, SR structure in *unc-89(sf22)* vs. wild type. Scale bar, 10 μ m.

TBA-1-HA

**Wild
type**

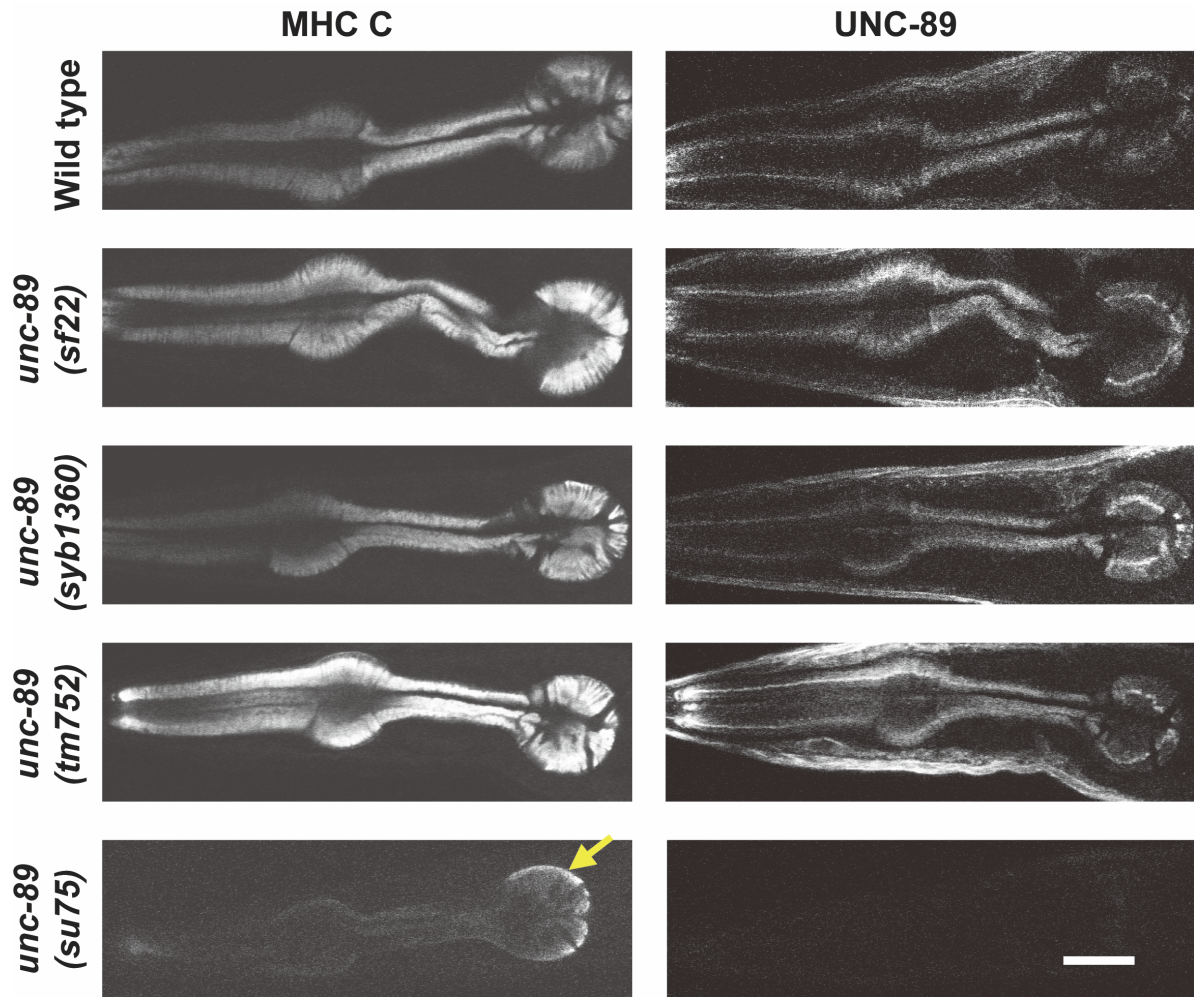


***unc-89
(sf22)***



Supplementary Figure 5. The PK2 KtoA mutation does not affect the organization of microtubules.

Confocal images of portions of body wall muscle cells immunostained with antibodies to HA to determine the localization of TBA-1-HA, an α -tubulin with an HA tag expressed using a promoter from a muscle gene (*myo-3*). There is no significant difference in the localization of TBA-1-HA in *unc-89(sf22)* vs. wild type. Scale bar, 10 μ m.



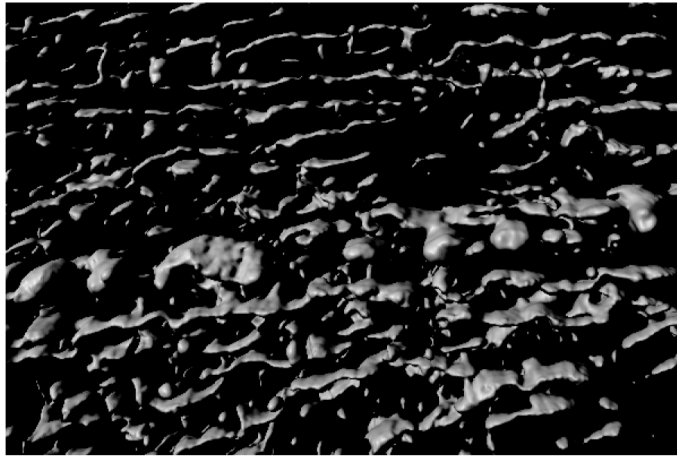
Supplementary Figure 6. The PK2 KtoA mutation does not affect the organization of the myofilament lattice of pharyngeal muscle.

Wild type and *unc-89* mutant alleles were co-immunostained with antibodies to the pharyngeal muscle-specific myosin heavy chain MHC C, and to UNC-89. The pharynx of wild type shows radially oriented thick filaments (MHC C imaging), and UNC-89 localized to the middle of these filaments. Note that *unc-89(su75)*, which does not express the giant UNC-89 isoforms shows arc-like thick filaments (yellow arrow) located at the periphery of the terminal bulb, and no staining with anti-UNC-89. All previously characterized *unc-89* mutants show these arc-like filaments, except for *unc-89(tm752)*, which lacks expression of all kinase-containing isoforms, and shows a normal localization of myosin and UNC-89. Note that the two independently isolated PK2 KtoA mutants, *sf22* and *syb1360*, have a normal myofilament lattice and localization of UNC-89. Scale bar, 10 μ m.

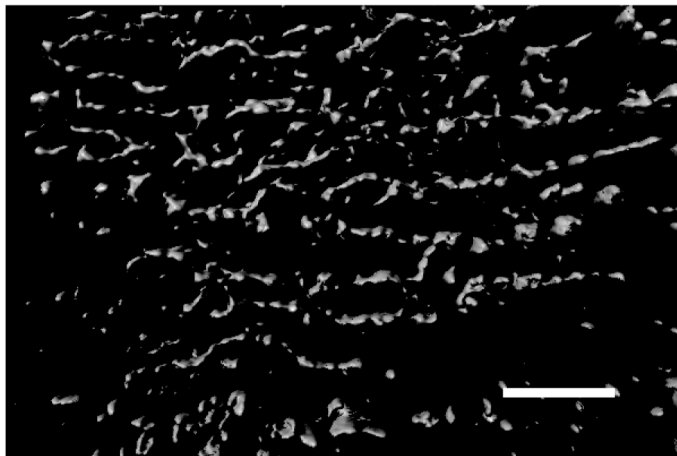
ATP5A (SIM)

3D rendering

unc-22
(*sf21*)

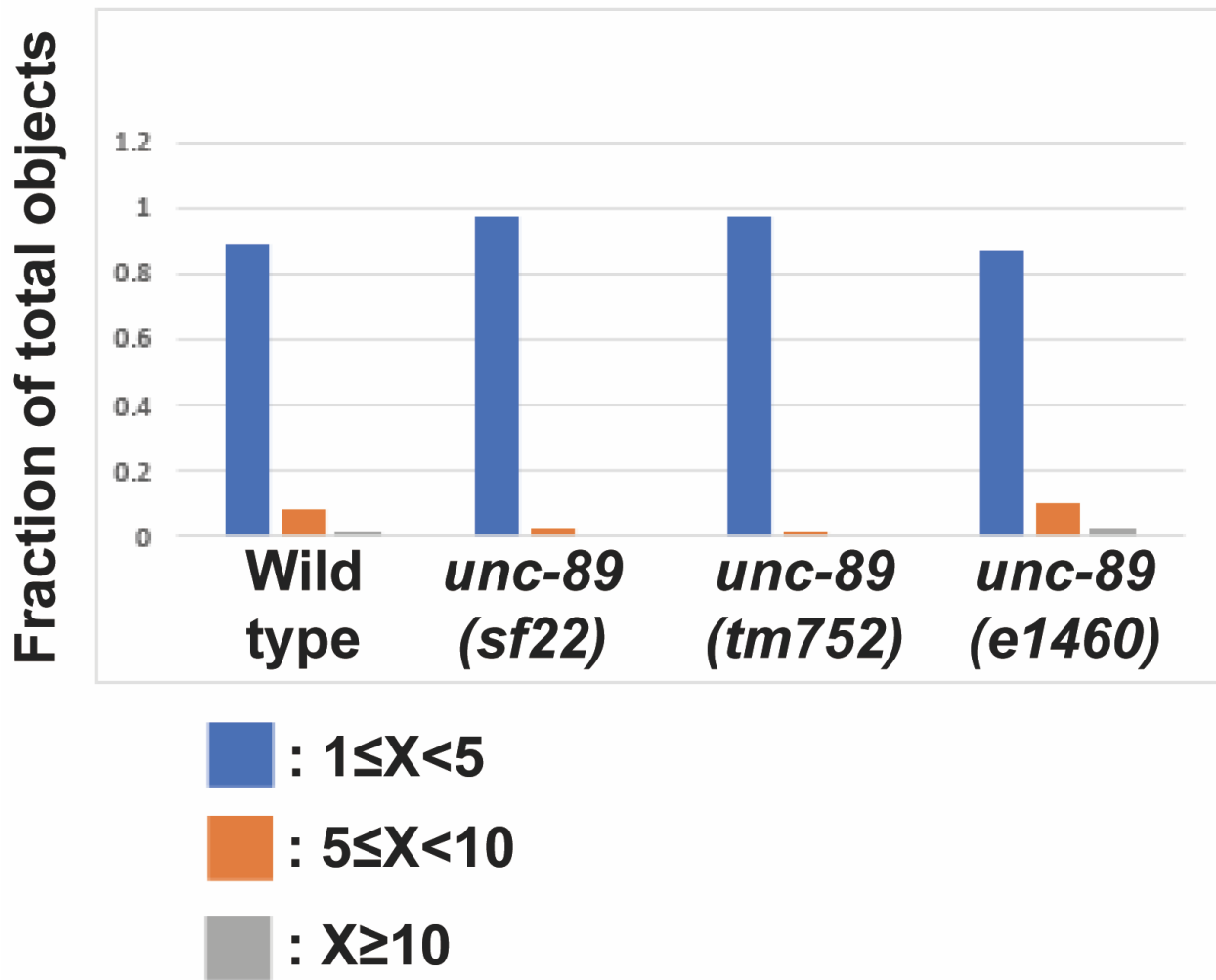


unc-22
(*e105*)



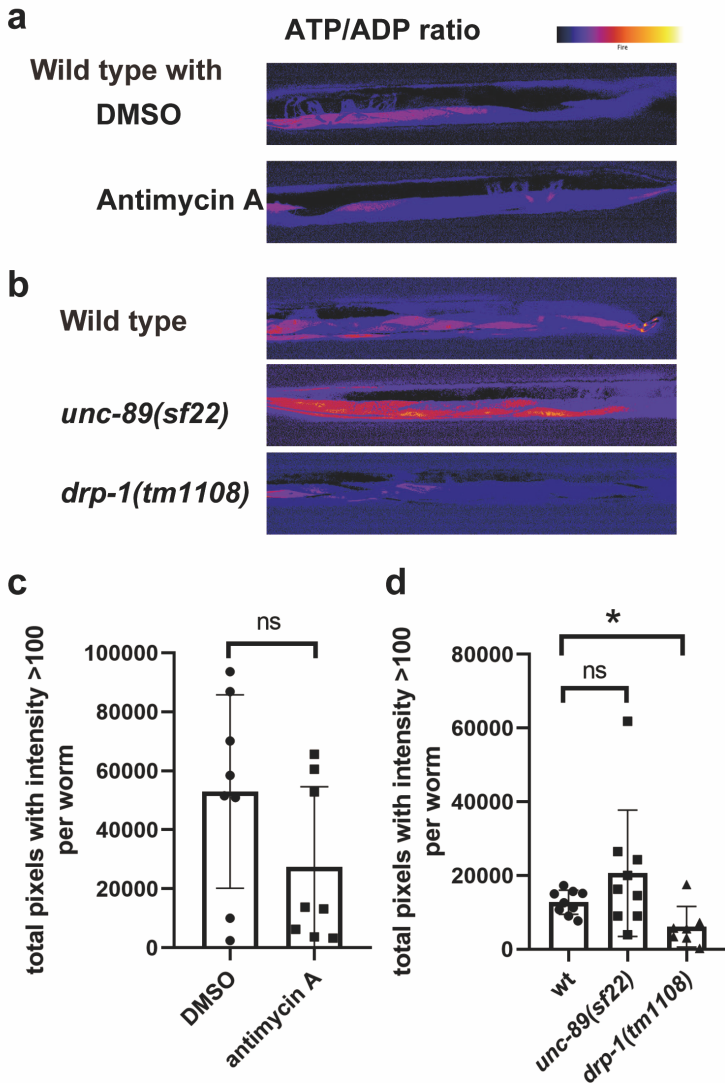
Supplementary Figure 7. Two unusual *unc-22* mutants that move faster than wild type show normally organized, not fragmented, mitochondria.

unc-22(sf21) has an inactivating KtoA mutation in the protein kinase domain of twitchin². *unc-22(e105)* has a missense mutation in Ig7 of twitchin but also displays faster whole animal locomotion. In both mutants, the muscle mitochondria are organized as long thin wavy lines roughly parallel to the muscle A- and I-bands. Images are 3D renderings of SIM images of muscle mitochondria immunostained with anti-ATP5A. Scale bar, 5 μ m.



Supplementary Figure 8. Quantitation of mitochondrial length from 3D reconstructions of SIM images.

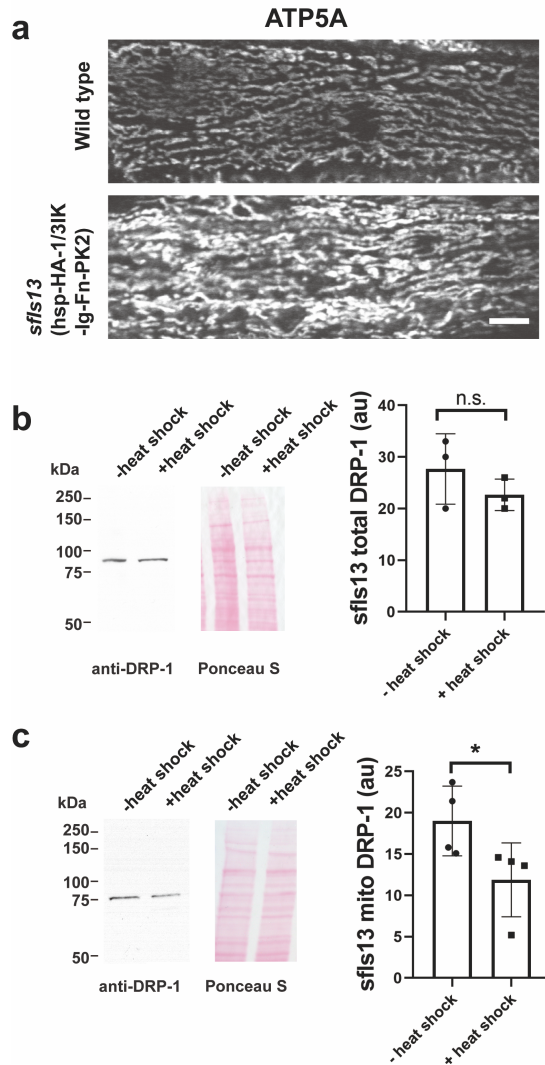
The longest axis of each anti-ATP5A-staining object (mitochondrion) was determined using Imaris software. The mitochondria were placed into 3 bins: $1 \leq x < 5 \mu\text{m}$, $5 \leq x < 10 \mu\text{m}$, and $x \geq 10 \mu\text{m}$.



Supplementary Figure 9. The ATP/ADP ratio might be elevated in body wall muscle of a PK2 KtoA mutant.

- a. A transgene was created in a wild type background that expresses the PercevalHR fluorescent biosensor in body wall muscle and crossed into the indicated mutant strains. The ATP/ADP ratio was measured by ratiometric imaging. a and b. Representative images from the indicated strains. As expected, the complex III inhibitor antimycin A, and the *drp-1* mutant each reduce this ratio. Note that *unc-89(sf22)* shows an increase in the ATP/ADP ratio. c and d. Quantitation of results shown in a and b, as described in materials and methods. Statistical significance was assessed using an unpaired t test with Welch's correction. For c, comparing DMSO vs. antimycin A,

although not reaching significance, $p=0.0563$. For d, comparing wild type (wt) and *unc-89(sf22)*, although not reaching significance, $p=0.1046$; comparing wild type and *drp-1(tm1108)*, $p=0.0100$.



Supplementary Figure 10. Overexpression of PK2 results in more mitochondrial clumping and a reduction in mitochondrially-associated DRP-1.

a. Confocal images of several body wall muscle cells immunostained with antibodies to ATP5A to reveal the morphology of mitochondria. Wild type animals show the typical long wavy lines often described as tubular. In contrast, a transgenic animal, *sfIs13*, expressing from a heat shock promoter, a portion of UNC-89 containing PK2 shows more clumping. b. Western blot showing the level of DRP-1 before and after heat shock induced expression of PK2 from *sfIs13*. Note that the level of total DRP-1 does not change. c. Western blot showing the level of DRP-1 associated with isolated mitochondria before and after heat shock induced expression of PK2 from *sfIs13*. Note that the level of mitochondrially-associated DRP-1 decreases upon increasing the expression of PK2.

PHX1195 *unc-89(syb1195)*

Synonymous mutations are labeled in blue.

PCR primers and sequencing primers:
BG12-Seq-s:GAGTCACTGCACAGAATGGA
BG12-Seq-a:TAGTTTCACGACCCAACTAC

>BG12-syb1195

GAGTCACTGCACAGAATGGATTCCGGTCTAGGGCTCCCATCATTGAGTAGCAGAATTGTTCA
AACTCACGGAAAAGGAGCACCAAAGTTGCAAATTGATGTTTTGAAATCCGAGATTCTGACTG
AATGTTGTTTTCAATGCCTCAAAGTCTACAAATCAATTAGGAGGAATTTCCGAGGAAAAGTGA
AGAGGATTCGGAGGCAAGAACGGCAAATGAAGATATGAAATCAAATCTGCAATTGCAAAC
GATGATCCAACAGGACGGTTCCAGGtaagggacactcaggaataaaaagaaagtcagtgtgaaatttcctttata
ctgggaataaattaggcaaaatccctactaacaatatccatattttgtacactgaaagtaattctaaacctgtatttataacgagacatct
ataaattttctagcagaaatttgccccaagaaaattttttgaataatttttaaagagttttttgggtgtttgggggtgagttcataatac
atatataattaatacaattttgcactcacaagtaaaaaatagttctgtggcattttaaaattaaattatatacatttttcattcactattccac
ataaaattgttcagATCGGTGGTCTCAAGTTCAAGGGACGTTTCTCTGTGATCCGCGACGCCGTC
GATTCCACAACAGAAGGTCACGCCATTGCGCTGTGCCATTTCGTCATCCATCGTCTGAAG
CGATCTCAGAGTATGAATCGCTTCGTGATGGTCAGCATGAAATGTTCAACGCCTTATCGC
CGCATTCAATAACTCCAATTTCTTGTATCTATTATCGGAAAGACTCTACGAAGATGTGTTTTT
TCGTTTTGTGTTCAACGATTATTATACAGAAGAACAAGTTGCATTGACAATGAGACAAGTCA
CTTCGGCACTTCATTTCTTGCATTTCAAAGGgtgagcttaacagttataacagttataaattcctaattctaatttt
gatttttagAATTGCCCATCTTGATGTGAATCCACACAACATAATGTTCCAATCAAACGTTAGTTG
GGTCGTGAAACTA

PHX1360 *unc-89(syb1360)*

Synonymous mutations are labeled in blue.

PCR primers and sequencing primers:
BG12-Seq-s:AACTCACGGAAAAGGAGCAC
BG12-Seq-a:TAGTTTCACGACCCAACTAC

>BG12-syb1360

AACTCACGGAAAAGGAGCACCAAAGTTGCAAATTGATGTTTTGAAATCCGAGATTCTGACTG
AATGTTGTTTTCAATGCCTCAAAGTCTACAAATCAATTAGGAGGAATTTCCGAGGAAAAGTGA
AGAGGATTCGGAGGCAAGAACGGCAAATGAAGATATGAAATCAAATCTGCAATTGCAAAC
GATGATCCAACAGGACGGTTCCAGGtaagggacactcaggaataaaaagaaagtcagtgtgaaatttcctttata
ctgggaataaattaggcaaaatccctactaacaatatccatattttgtacactgaaagtaattctaaacctgtatttataacgagacatct
ataaattttctagcagaaatttgccccaagaaaattttttgaataatttttaaagagttttttgggtgtttgggggtgagttcataatac
atatataattaatacaattttgcactcacaagtaaaaaatagttctgtggcattttaaaattaaattatatacatttttcattcactattccac
ataaaattgttcagATCGGTGGTCTCAAGTTCAAGGGACGTTTCTCTGTGATCCGCGACGCCGTC
GATTCCACAACAGAAGGTCACGCCATTGCGCTGTGCCATTTCGTCATCCATCGTCTGAAG
CGATCTCAGAGTATGAATCGCTTCGTGATGGTCAGCATGAAATGTTCAACGCCTTATCGC
CGCATTCAATAACTCCAATTTCTTGTATCTATTATCGGAAAGACTCTACGAAGATGTGTTTTT
TCGTTTTGTGTTCAACGATTATTATACAGAAGAACAAGTTGCATTGACAATGAGACAAGTCA
CTTCGGCACTTCATTTCTTGCATTTCAAAGGgtgagcttaacagttataacagttataaattcctaattctaatttt

gatttttagAATTGCCCATCTTGATGTGAATCCACACAACATAATGTTCCAATCAAAAACGTAGTTG
GGTCGTGAAACTA

PHX6586 *ucp-4*(*syb6586*)

Synonymous mutations are labeled in blue.

PCR primers and sequencing primers:

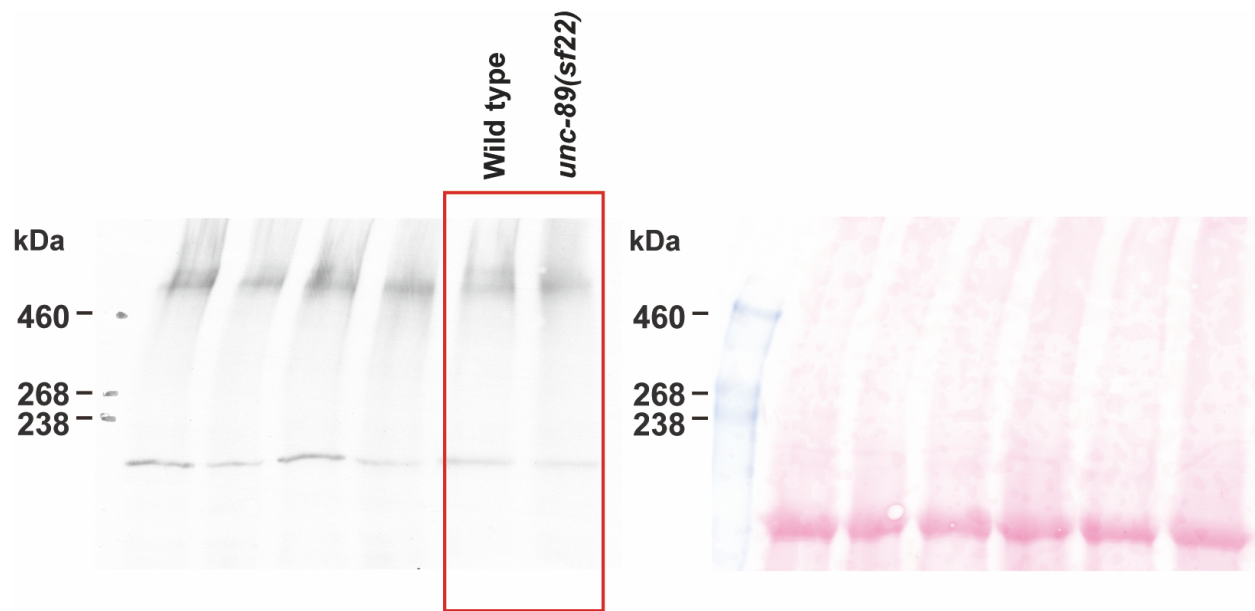
BG39-seq-s:CATTGTCCGTACAAATGGTA

BG39-seq-a:ACAAATAATAGTTCCACCCG

>BG39-syb6586

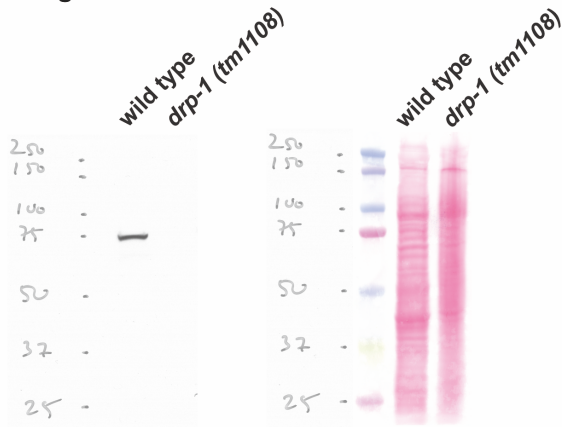
cattgtccgtacaaatggtataagttattgtatttgaaaacgtactttgaaaaaaaaatattttaagttctgcggaaatctattgtaa
aattttatattaaaactaacatatcaatttcagGATAATTGGCTAACTCATGCCGTTGCTAGTGCTTGTGCT
GGACTTGCTGCTGCCATTGTATCACTTCCATCAGATGTCGTTAAAACCTCGAATGATGGATCA
GATTCGGCACGAGCTGGACGCCAAAATgtttgcatcattgtttcgtttcatatttcaaattattgtatttcagGATGC
ATAAGAAAAATACGCATGTGGATCTATACAAAGGCGTCGTCGATTGCTACATAAAAAATTATC
AAAACGAAGGATTTTTCTCACTTTACAAAGGATTCCTTCCATCTTATATTCTGAATGGCTCC
GTGGTCTCTTACCTTCTGGGTCTCTACGAAGAGATTTCGTAATGGACTGGCGCTTCAAGT
TTCACCCATACGATGTTCCAGATTACGCTGGTGGATCTTACCCATACGATGTTCCAGATTA
CGCTGGTGGATCTTACCCATACGATGTTCCAGATTACGCTTAGtttgcttcataattcagttatagttttgct
taaaattgaattagttatagattttcagttatttttaattcatttaagtaagccacgggtattgtctttttctatgattttgacagataggaa
attattttgttgcgagcttccgtcaatcccattgtcttttttctaattacctgtgccatcttctccctttcgttgctcatagactctttcgggtattt
ttgcattatttttagcgttttcgaattgagatattcgtaattagatcagttgtatgttgacatttcgatatttaattatgtagcaatgcggtcgt
tgaaccgtgaaaatatttttagctgtataagttagcttacaattcttgaattcagatgaaactcgggtggaactattttgt

Supplementary Figure 11. Description of CRISPR/Cas9 generation of *unc-89*(*syb1195*), *unc-89*(*syb1360*), and *ucp-4*(*syb6586*).

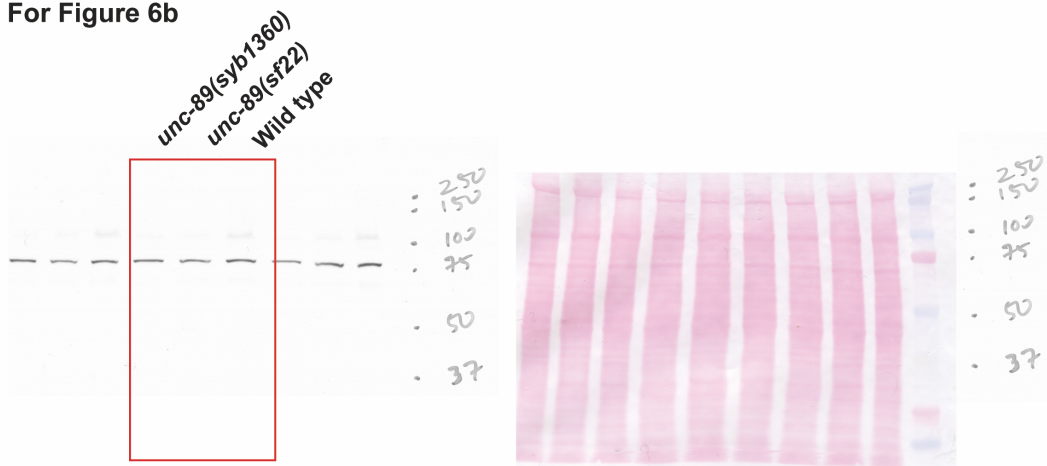


Supplementary Figure 12. Uncropped and unedited western blot images used to prepare the western blot shown in Figure 1d. The western image is shown on the left, and the Ponceau S staining of the blot including the molecular weight markers, is shown on the right. The red rectangle indicates the portion presented in Figure 1d.

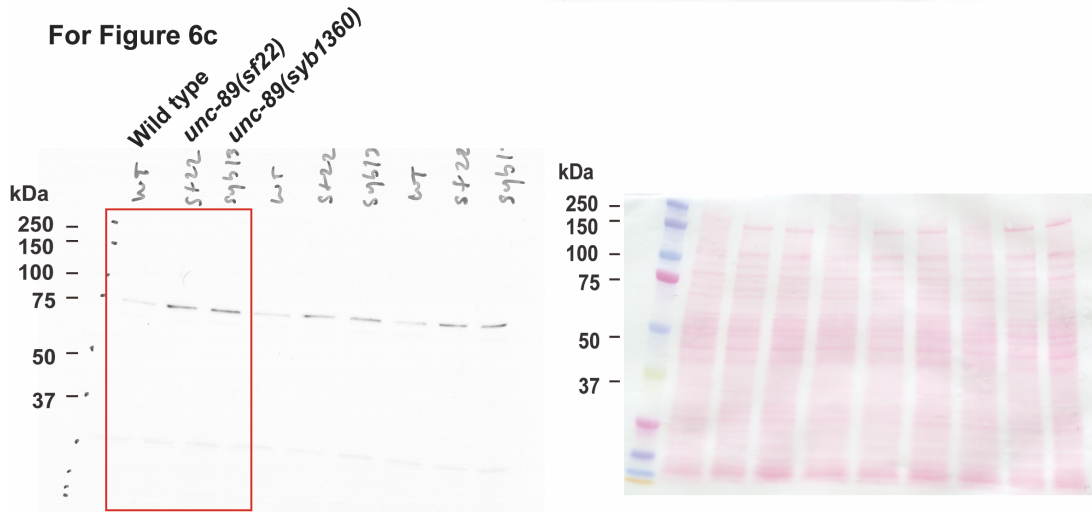
For Figure 6a



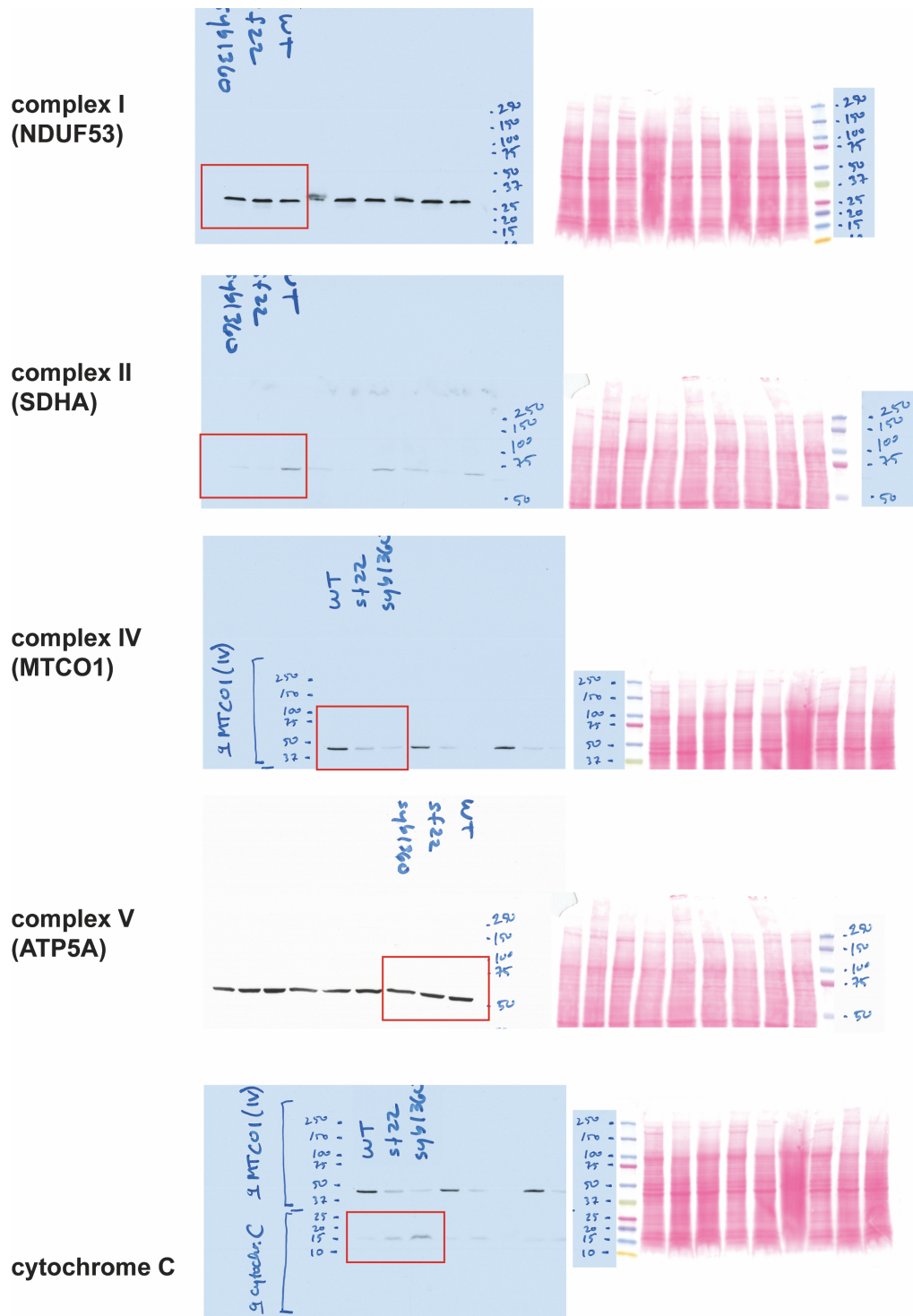
For Figure 6b



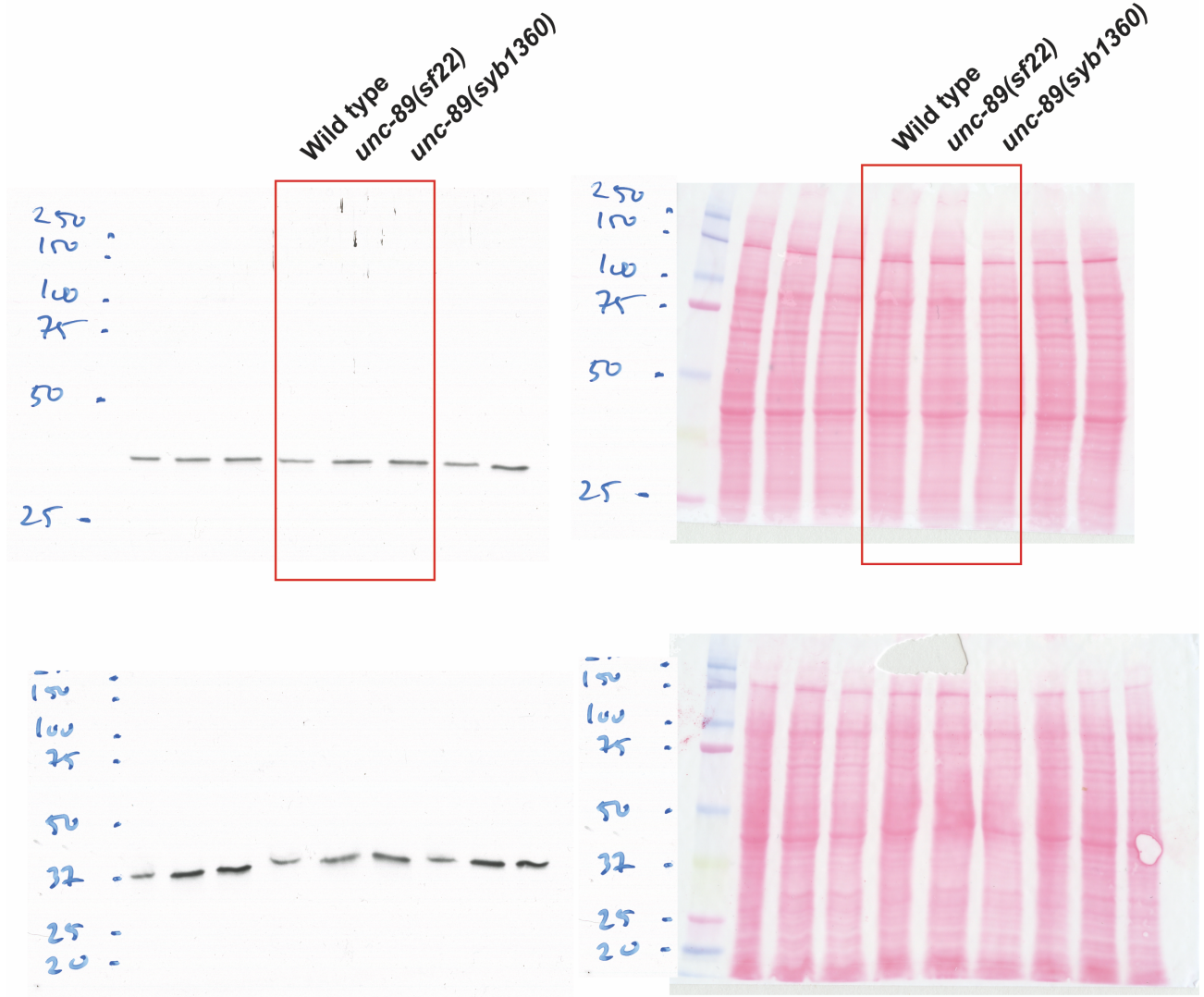
For Figure 6c



Supplementary Figure 13. Uncropped and unedited western blot images used to prepare Figure 6a, b and c. For each part, the western images are shown on the left, and the Ponceau S staining of the blots, and including the molecular weight markers, are shown on the right. Red rectangles indicate the regions presented in Figure 6b and c.

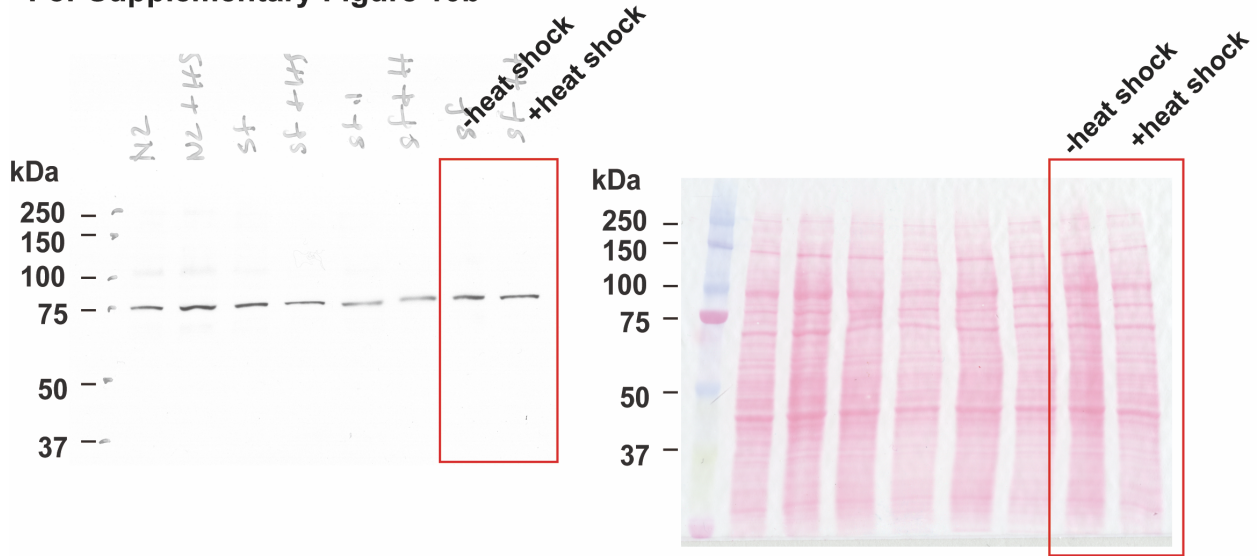


Supplementary Figure 14. Uncropped and unedited western blot images used to prepare Figure 8c and d. For each row, the results of the antibody reaction are shown on the left, and the Ponceau S staining of the blot is shown on the right. The red rectangles indicate the regions presented in Figure 8c.

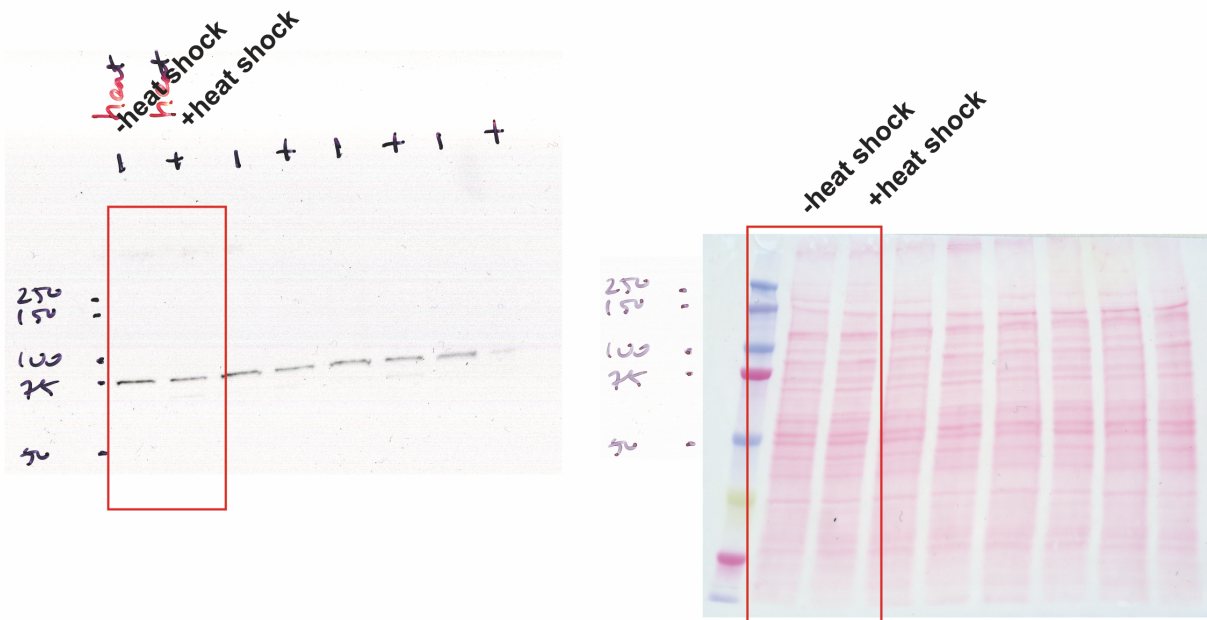


Supplementary Figure 15. Uncropped and unedited western blot images used to prepare Figure 10a and b. The results of the antibody reaction are shown on the left, and the Ponceau S staining of the blot is shown on the right. The red rectangle indicates the region presented in Figure 10a.

For Supplementary Figure 10b



For Supplementary Figure 10c



Supplementary Figure 16. Uncropped and unedited western blot images used to prepare Supplementary Figure 10b and c . The results of the antibody reactions are shown on the left, and the Ponceau S staining of the blots are shown on the right. The red rectangles indicate the regions presented in Supplementary Figures 10b and c.

Supplementary References

1. Hu LY, Kontrogianni-Konstantopoulos A (2013). The kinase domains of obscurin interact with intercellular adhesion proteins. *FASEB J* 27, 2001-2012
2. Matsunaga Y, Hwang H, Franke B, Williams R, Penley M, Qadota H, Yi H, Morran LT, Lu H, Mayans O, Benian GM (2017). Twitchin kinase inhibits muscle activity. *Mol Biol Cell* 28, 1591-1600